IMAGING THE VELOCITY FIELD IN FILM SPLITTING FLOWS OF DILUTE POLYMER SOLUTIONS

Melisa Yvone Zambrano Becerra
Department of Mechanical Engineering - Pontifícia Universidade Católica de Rio de Janeiro
R. Marques de São Vicente 225 - Gávea, Rio de Janeiro, RJ, Brasil.
melisa@mec.puc-rio.br

Marcio da Silveira Carvalho
Department of Mechanical Engineering - Pontifícia Universidade Católica de Rio de Janeiro
R. Marques de São Vicente 225 - Gávea, Rio de Janeiro, RJ, Brasil.
msc@mec.puc-rio.br

Luis Fernando Alzuguir Azevedo
Department of Mechanical Engineering - Pontifícia Universidade Católica de Rio de Janeiro
R. Marques de São Vicente 225 - Gávea, Rio de Janeiro, RJ, Brasil.
lfaa@mec.puc-rio.br

Abstract.
Roll coating is widely used to apply a thin liquid layer to a continuous substrate. The coated film quality and thickness depend of the behavior of the film split. When the roll speed is too fast, the gap is too small or the liquid viscosity is too high, the film is not uniform in the cross-web direction and filaments are formed, which are communly called "ribbing". Viscoelastic liquids can drastically change the nature of the flow near the free surfaces of the coating bead. The onset of the instabilities occurs at much lower speeds than Newtonian case. Recent theorical predictions have shown that when viscoelastic forces are strong near the meniscus, the recirculation present in Newtonian flow completely dissapears. In this work, film splitting flows between a stationary plate and rotating roll are analyzed experimentaly by visualizing the free surface configuration and measuring the velocity field using the Particule Image Velocimetry (PIV) technique. Dilute polymer solutions are used in order to evalute the effect of the viscelastic behavior on the flow. The goal is to confirm the theorical prediction on the effect of liquid viscoelasticity on the streamline pattern and on the stability of the free surface.

Keywords: *Roll coating, rheology, viscoelastic liquids, free surface, PIV.*

1. Introduction

Roll coating is a common method in the manufacture of a wide variety of products as membranes, galvanized steel, paper, fotografic films and many others. It applies a thin liquid layer to a continous substrate. At low speed the flow is two-dimensional and steady; as the roll speed is raised, the two-dimensional flow becomes unstable and is replaced by steady three-dimensional flow which results in more or less regular stripes in the machine direction. This type of the instability is commonly called *ribbing*; it can limit the speed of the process if a smooth film is requerid as final produtc.

The film splitting flow of a Newtonian liquid exiting from two rotating rolls and the associated instability have been studied extensively. Pearson et al. (1960) showed that the adverse pressure gradient near the film-split meniscus necessary to decelerate the flowing liquid destabilizes the free surface, where surface tension has a stabiling effect. A critical value of the ratio between these two forces, i.e., capillary number $Ca = \mu V/\sigma$, marks the onset of the free surface nouniformity. Here, μ is the liquid viscosity, σ its surface tension, and V is the mean roll speed.

In practice, coating liquids often contain polymers. Viscoelastic behavior can drastically change the nature of the flow near the free surface of coating beads. The extension-domineted deformation that occurs in this flow zone leads to changes in the forces balance at the meniscus. In the particular case of forward roll coating, it has been shown experimentally that when minute amounts of flexible polymer are present, the onset of the three-dimensional instability that leads to regular stripes in the machine direction (ribbing) occurs at much lower speeds than in the Newtonian case as shown in Fig.1. Bauman et al. (1982) experimentally tested the effect of certain polymer additives on the ribbing instibility. They observed that the critical speed at which ribbing first appeared was lower than in the case of a Newtonian liquid. Carvalho et al.(1994), and later Dontula et al. (1999), analyzed experimentally the film splitting flow of aqueous solutions of PEG (polyethilane glycol) and PEO (polyethelene oxide). They concluded that minute amounts of flexible polymer lowered drastically the critical speed at which the three-dimensional instability occurs. Lopez et al. (2002) studied experimentally the instability of non-Newtonian flow between two non-concentric cylinders. They used two aqueous polymer solutions with similar shear-thinning behavior but different elastic characteristics, i.e., Xanthan (inelastic) and Polyacrylamide (elastic). With the elastic (Polyacrylamide) solution, the critical capillary number for the instability dropped with growing polymer concentration by up to one order of magnitude compared to the Newtonian case. With the Xanthan solution,

the critical capillary number decreased only slightly. The resulting three-dimensional pattern of the free surface is also a strong function of the liquids. Owens et al. (2004) analyzed the effect of polymer additivies on the stability of film splitting flows and on mist formation.

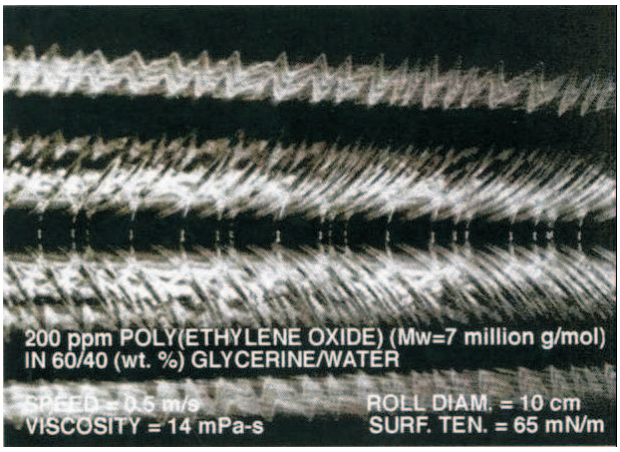

Figure 1. Three-dimensional periodic flow in forward roll coating film splitting (from Carvalho et al. 1994).

Accurate theorical predictions of the onset of ribbing when viscoelastic liquids are used is still not available. The mechanisms by which the liquid elasticity makes the flow unstable at Capillary numbers much lower than Newtonian was revealed by recent theoretical predictions of Zevallos et al. (2004) that showed how the stress field changes with rising liquid elasticity (Weissenberg number), leading to the formation of an elastic stress boundary layer attached to the free surface. The high stress downstream of the flow splitting stagnation point pulls liquid away from the recirculation attached to the free surface and completely change the flow characteristics in that region. The evolution of the streamlines at $Ca = 0.2$ and normal stress along the streamlines as the liquid becomes more elastic predicted by Zevallos et al. (2004) is presented in Fig. 2. At high Weissenberg number, the recirculation zone, present in the Newtonian flow completely dissapears. One of the goals of this work was to confirm the theoretical predictions of Zevallos et al. (2004) on the effect of the liquid viscoelasticity on the streamline pattern and on the stability of the free surface with respect to three-dimensional disturbances.

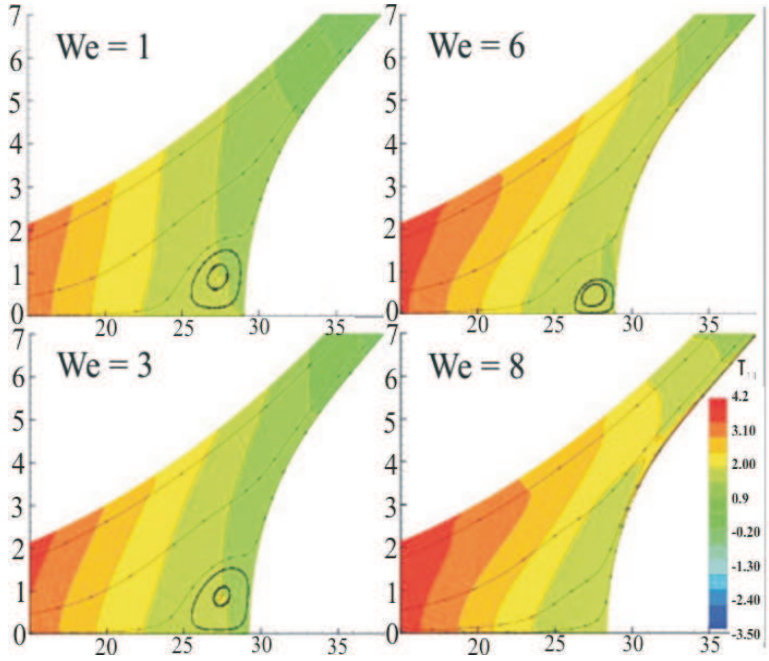

Figure 2. Evolution of the streamlines and normal stress component along the strealines as Weissembreg number grows at Ca=0.2 (from Zevallos et al. 2004).

2. Experimental Analysis

2.1 Setup

The experiments were conducted in the test section shown schematically in Fig. 3. It consisted of a stationary glass plate and a rotating roll (diameter of 20 cm). Liquid was picked out of a pan and a liquid bead was formed in the small space between the plate and the roll. A meniscus was formed in the region where the liquid dettaches from the plate and forms a film on the roll surface. The test section was specially designed to allow visualization of the coating bead from two different angles: a frontal view, through the glass plate, and a lateral view. The front view was used to determine the configuration of the static contact line on the plate and consequentely the onset of the three-dimensional configuration of the meniscus. The lateral view was used to visualize the flow pattern and the meniscus configuration and to measure the velocity field near the free surface using the Particle Imaging Velocimetry technique.

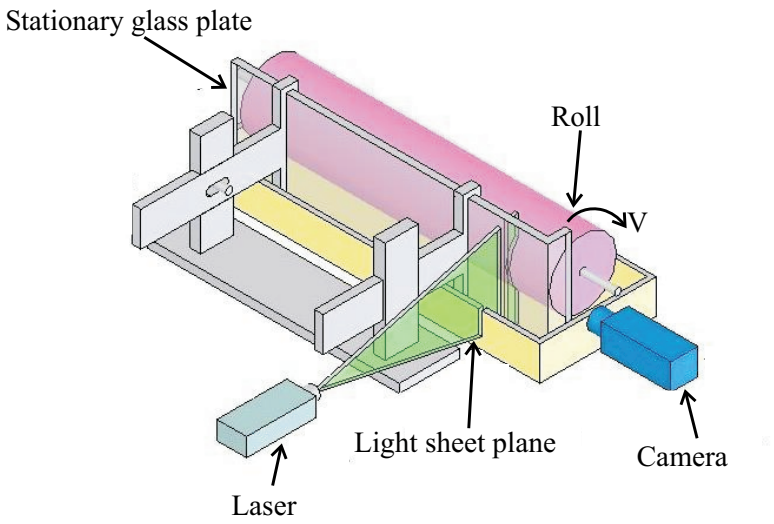

Figure 3. Experimental setup.

The operating parameters that were controled during the experiments were the gap between the roll and the stationary plate H_0, the roll speed *V* and the liquid properties. For Newtonian liquids, the important dimensionless parameters are:

- Gap-to-roll radius ratio: $\frac{H_0}{R}$
- Capillary Number: $Ca \equiv \frac{\eta V}{\sigma}$

Where η is the liquid shear viscosity, and σ its surface tension.

2.2 Coating solutions and their rheological properties

Different solutions of PEG (poly-ethelene glycol, molecular weight 6x10^3 g/mol) and PEO (poly-ethelene oxide, molecular weight 8x10^6 g/mol) in water were used in the experiments. Dontula et al. (1999) proposed this kind of solutions to study the role of elasticity in coating and other free surface flows. These solutions are transparent and behave as Boger liquids. The solution of low molecular weight PEG in water was used as the "solvent" to all liquids tested. Because of the low molecular weight, the solution of PEG in water is Newtonian. The concentration of the PEG was fixed at 30 wt$\%$, which yeilded a viscosity of approximately 30 cP. The addition of small quantities of the high molecular weight PEO made the solutions elastic. The concentration of PEO varied from 0 to 0.1 wt$\%$.

The rheological characterization of the solutions was made in shear and extension-dominated flow. The rheological properties in shear were obtained using a rotational rheometer (ACER, Rheometrics Inc.) with a cone-and-plane fixture and a Cannon-Fenske glass capillary rheometer, to measure accurately the shear viscosity at low shear rate. The shear viscosity of all solutions tested is independent of the shear rate, as shown in Fig. 4, indicating that at this level of concentration of PEO, the solutions were in the dilute regime. The apparent extensional viscosity measurements were made using an opposed-nozzle rheometer (RFX, Rheometrics Inc.). Several nozzle diameters were used in order to cover the range of nominal extensional rate reported. The results are presented in Fig. 5. For the Newtonian solution (0$\%$ PEO), the apparent extensional viscosity is virtually independent of extensional rate, and the Trouton ratio (η_e/η_s) is approximately 3.2. The apparent extensional viscosity rises as the concentration of the high molecular weight polymer increases. The maximum Trouton ratio of the 0.05 wt$\%$ PEO solution was approximately 16.

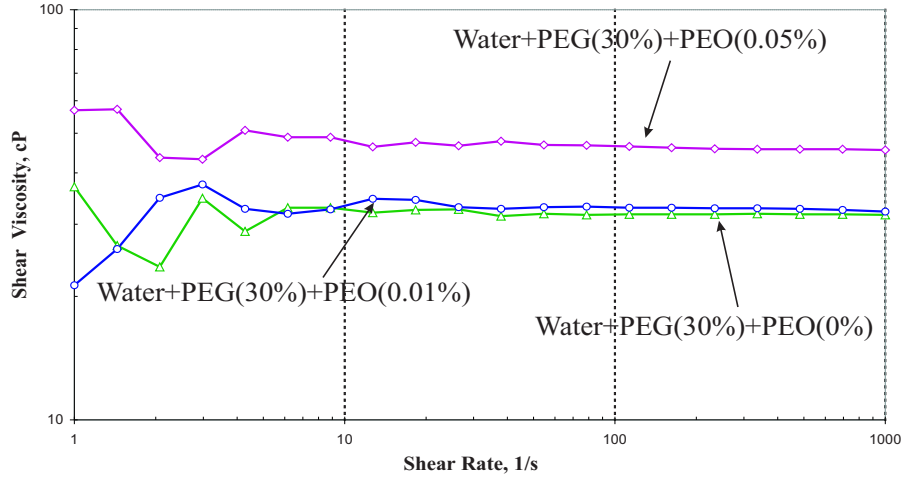

Figure 4. Shear viscosity dependence on shear rate.

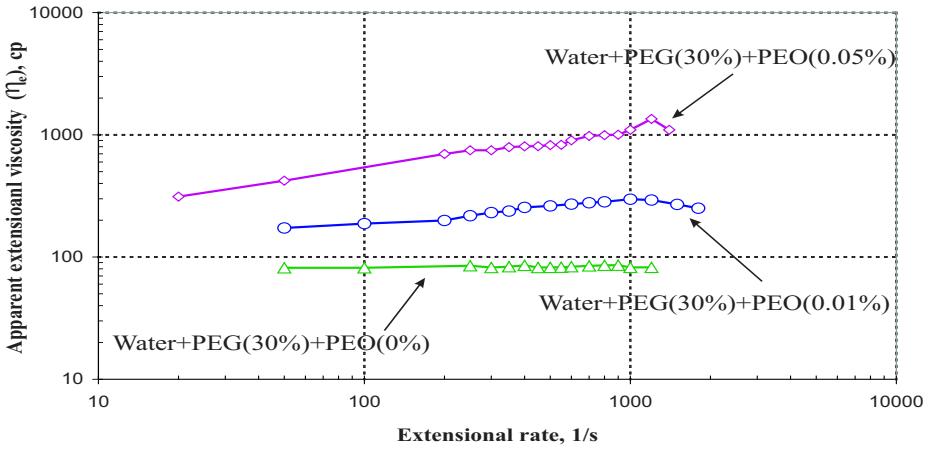

Figure 5. Apparente extensional viscosity dependence on extensional rate.

The apparent extensional viscosity gives a qualitative measure of the elastic forces of the liquid, however, it is hard to evaluate a relaxation time based on these measurements. The relaxation time of the different viscoelastic solutions tested were estimated by taking the ratio of the polymer contribution to the total viscosity and the elastic modulus of the polymer, which is a function of the polymer concentration and its molecular weight. Table 1 shows these calculation. Because the solutions are dilute, the relaxation time is not a function of the concentration of the polymer. The viscoelastic effects in a flow are characterized by three different dimensionless parameters:

- Weissenber number: $We \equiv \frac{\lambda V}{H_0}$, which is a function of the relaxation time of the liquid.
- Solvent to total viscosity ratio: $\beta \equiv \frac{\eta_s}{\eta_s+\eta_p}$ which is a function of the concentration of the polymer.
- Extensibility parameter, which is a function of the polymer molecule structure and its molecular weight.

The difference between the viscoelastic solutions tested here was the concentration of the high molecular weight polymer. Because all solutions were in the dilute regime, the extensibility parameter and the relaxation time were the same for all liquids. In this case, at the same gap and roll speed, the viscoelastic effects were characterized only by the solvent-to-total viscosity ratio.

PEG $(wt\%)$	PEO $(wt\%)$	c (Kg/m^3)	η_s $(mPa.s)$	η_o $(mPa.s)$	$(\eta_o - \eta_s)/\eta_s$	G (Pa)	λ (seg)
30	0	0	26.25	26.25	0	0	0
	0.01	0.1047	26.25	28.01	0.0670	0.0325	0.054
	0.05	0.5270	26.25	34.50	0.3143	0.1632	0.0505
	0.1	1.0545	26.25	42.96	0.6366	0.3267	0.0511

Table 1. Relaxation time of the different PEO concentrations .

2.3 Velocity measurements

The velocity field near the free surface was obtained in the experiments. A Particle Image Velocimetry system was employed to obtain the desired flow characteristics. In this technique an extensive region of the flow is illuminated by a pulsed sheet of laser light of elevated intensity, revealing the image of small tracer particles previously distributed in the fluid. A digital camera mounted orthogonaly to the light sheet records the position of the tracer particles at two close instants. A synchronization circuit coordinates the laser pulse with the camera capture, so that the two images are registered in consecutive frames. The particle displacements are determined by analyzing small sub-regions of the image (interrogation spots) and cross-correlating the image intensity distribution in the two frames. This process yields the mean particle displacement for each interrogation spot. The instantaneous velocity field is obtained by dividing the instantaneous displacement field by the time interval between laser pulses and by the magnification factor of the optical setup utilized.

Gomes et al (2000) developed a calibration experiment, for the system used in the present experiments, due to the complexity of the technique and to the elevated number of parameters that affect the results obtained. Moreover evaluated the relative importance of the several physical and computational parameters that affect the accuracy of the velocity measurements.Excellent comparison of measured and predicted results was obtained in this experiment with uncertainty level the order of 1%.

In the present experiments a PIV system manufactured by TSI Inc was utilized. This system employed a pair of integrated New Wave, frequency-doubled, Nd-YAG lasers capable of delivering up to 120 mJ of energy per pulse, at 15 Hz. The digital camera employed was a PIVCAM model 10-30 with resolution of 1000 x 1000 pixels using lens that yielded a magnification of 2.4x. The field of view was a square with sides of approximately 6 mm. Synchronization between the laser and the camera was controlled by a TSI model 60006 unit. The particle images were captured and processed by the Insight software developed by TSI Inc. The tracer particles used were polymer micro-spheres (polystyrene, polystyrebe divinilbenzene and other styrene copolymers) of $3\mu m$ diameter with red fluorescing. The interrogation area used to determine the velocity field was 32 x 32 pixels, which corresponded to $190\mu m$ x $190\mu m$. A filter of 570 nm was used in order to avoid the high intensity reflections from the free surface.

3. Results

The onset of ribbing was determined by observation of the contact line through the stationary glass plate at different gaps and different liquids. A sequence of images at rising capillary numbers at $H_0/R = 889\mu m$ is presented in Fig. 6. At low capillary number, the flow is two-dimensional and the position of the contact line does not vary in the transverse direction. At a critical capillary number, the meniscus becomes three-dimensional and periodic. The amplitude of the variation of the position of the contact line rises as the capillary number is increased above the critical value. The critical capillary number as a function of the distance between the roll and the plate for the different solutions used is presented in Fig. 7. The critical capillary number rises with the gap-to-roll radius ratio. At the same gap, the onset of the three-dimensional flow occurs at much smaller capillary number when the liquid is viscoelastic, as reported in the literature. As explained by Zevallos et al. (2004), the elastic stress boundary layer attached to the free surface pulls liquid out of the recirculation and changes the force balance at the interface. The normal tangential stress along the meniscus, which destabilizes the flow, grows as the viscoelastic properties of the liquid becomes stronger.

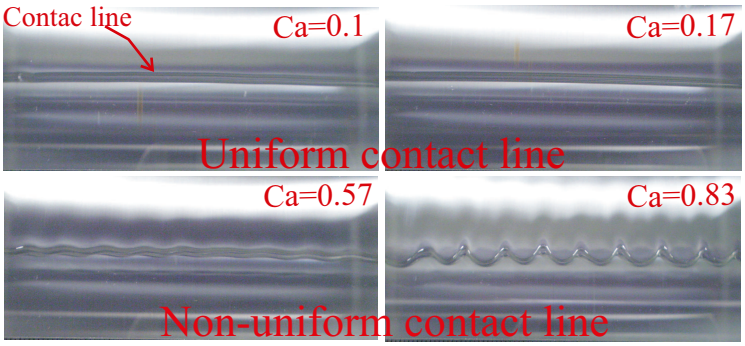

Figure 6. View of the contact line through the glass plate.

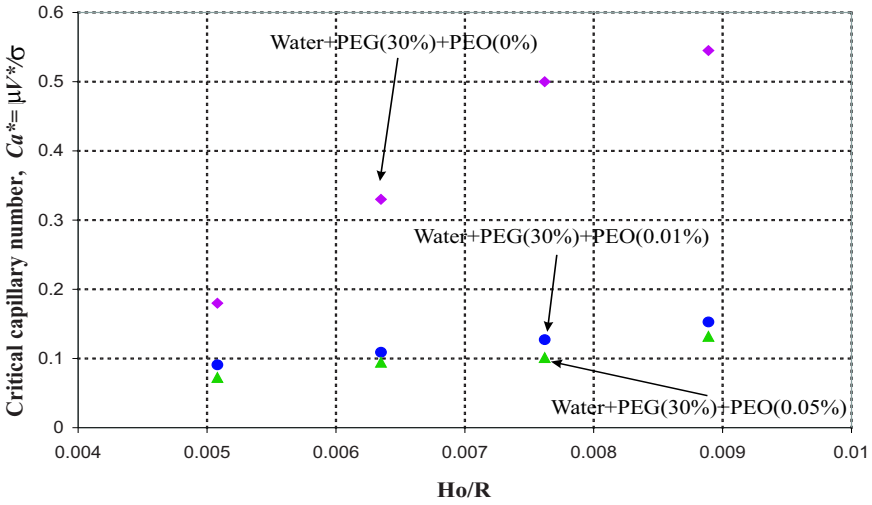

Figure 7. Critical capillary number for the onset of ribbing at several gaps.

Although all the process conditions were constant, the actual flow oscilated periodically with time. The reason for that was the small variation of the actual radius along the circunference of the roll from its specified value of $R = 10cm$. Because of the small clearance between the rotating roll and the plate, any small variation of the roll radius causes an appreciable variation on the gap. Consequentely, the meniscus position oscilated periodically and the flow was unsteady. In order to report the steady state values of the velocity field, a time-average of the velocity at each position was calculated. The sampling time was always larger than six revolution of the roll.

The velocity field near the free surface at $H_0 = 889\mu m$ and $Ca = 0.1$ for the Newtonian liquid is presented in Fig.8. There is a region of high velocity near the roll surface and a large recirculation attached to the free surface can be observed. The effect of the roll speed, represented in terms of the capillary number on the flow field is shown in Fig.9. As the capilary number rises, the recirculation region becomes smaller and smaller, until it almost vanishes at $Ca = 0.83$. The critical capillary number at this gap is approximately $Ca \approx 0.54$, and the flow field at the two highest capillary number shown in the figure are three-dimensional and what is shown in actually a slice of a flow field at a meniscus valey.

The effect of the viscoelastic forces on the flow field near the meniscus is illustrated in Fig.10. The gap-to-roll radius was $H_0/R = 889\mu m$ and the capillary number of all flow states shown was approximately $Ca \approx 0.18$. Each measurement was for a different polymer liquid, and consequentely different solvent-to-total viscosity ratio β. At this capillary number and gap-to-roll radius ratio, the Newtonian flow, i.e. $\beta = 1$, has a large recirculation attached to the free surface. As the polymer contribution to the total viscosity rises and consequentely β falls, the size of the recirculation diminishes until it vanishes at $\beta = 0.76$. These results validate the theoretical predictions of Zevallos et al. (2004).

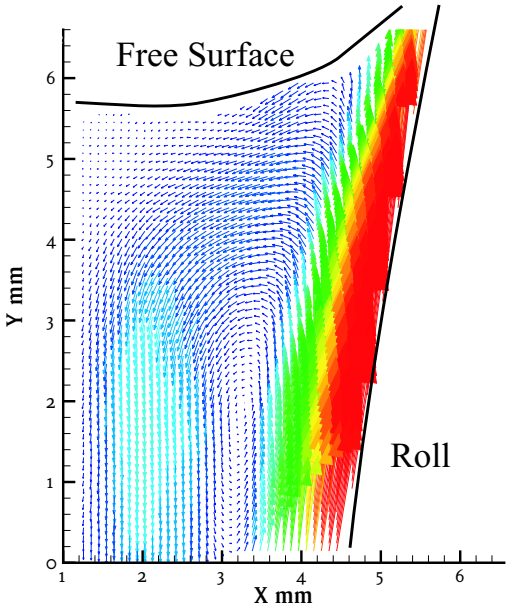

Figure 8. Velocity field for Newtonian liquid flow, $Ca = 0.1$ and $Ho = 889\mu m$

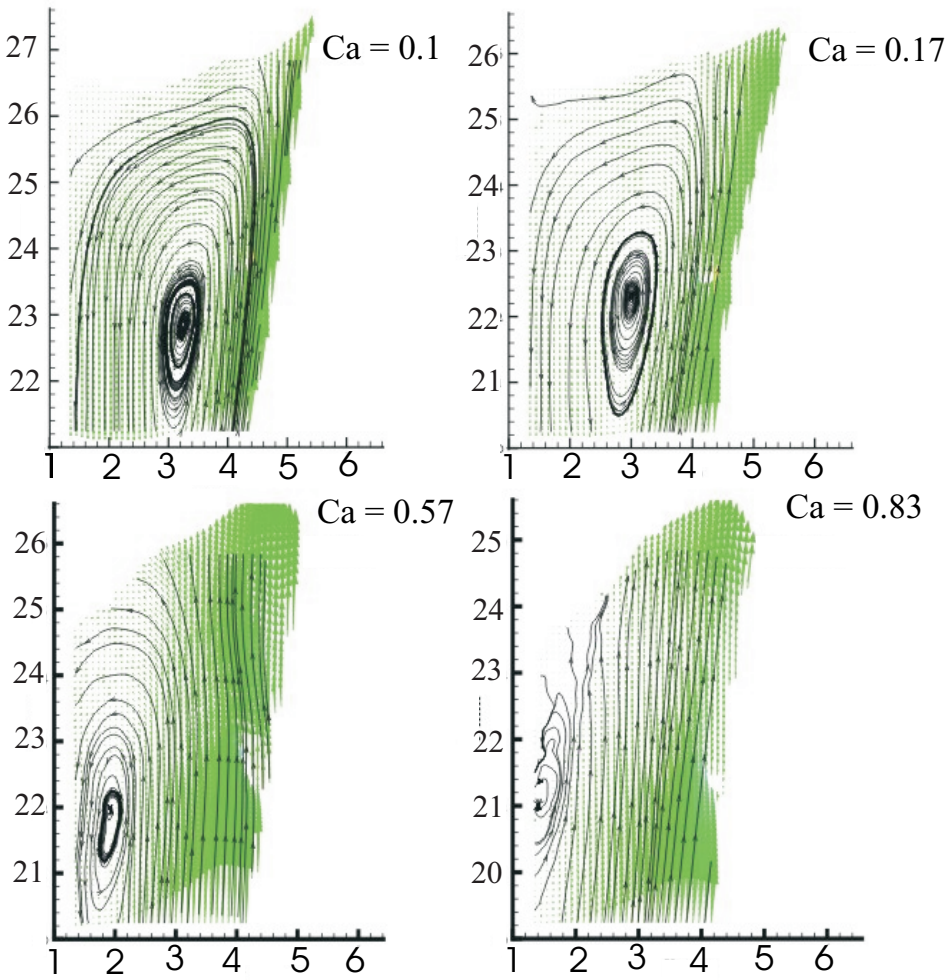

Figure 9. Velocity fields for Newtonian liquid flow, $Ho = 889\mu m$

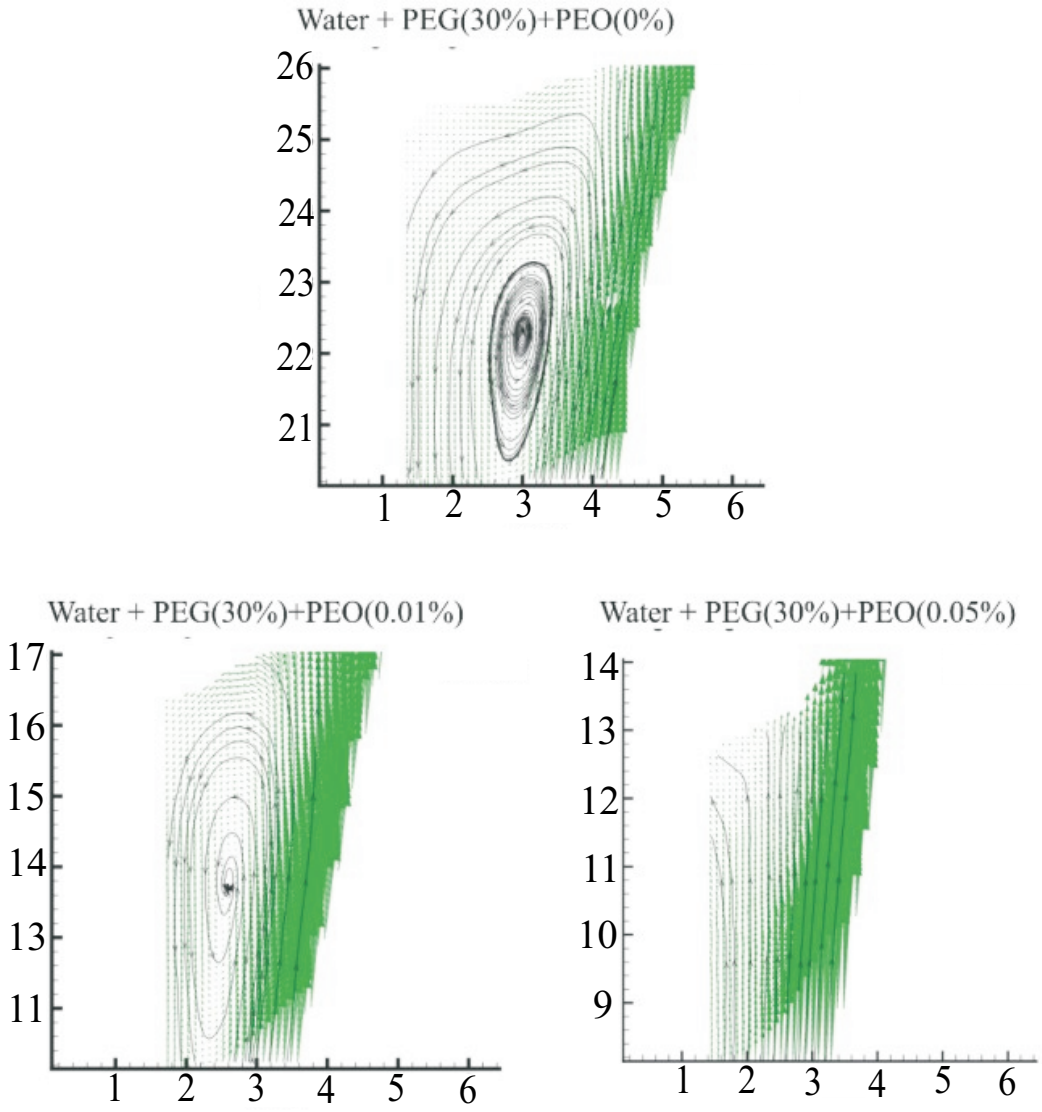

Figure 10. Velocity fields for Newtonian and viscoelastic liquid flow, $Ho = 889\mu m$

4. References

Bauman, T., Sullivan, T. and Middleman, S.,1989, "Ribbing instability in coating flows: effect of polymer additives", Chem. Eng. commun.,Vol.14, pp. 35-46.

Carvalho, M.S., Dontula, P. and Scriven, L. E., 1995, "Non-Newtonian effect on the Ribbing instabilities", TAPPI coanting conference, Dallas, USA.

Dontula, P.,1999, "Polymer solutions in coating flows", Ph.D Tesis, University of Minnesota, MN. Avalible from UMI, Ann Arbor, oredr number 99119386.

Gomes, B., Thompsom, R. and Azevedo, L., "Solid Body Rotation Flow for Particle Image Velocimetry Calibration", VIII Congresso Brasileiro de Engenharia e Ciência Térmica, ENCIT, Porto Alegre, novembro 2000 (CD-ROM)

Lopez, F.V.Pauchard, L., Rosen, M. and Rabaud, M.,2002, "Non-Newtonian effects on ribbing instability threshold", J. Non-Newtonian Fluid Mech., Vol.103, pp. 123-.

Owens, M.S., Scriven, L.E. and Macosko, C.W., 2004, "Rheology and control Minimizes Misting", ISCST Symposium.

Pearson,J.R.A., 1960, "The stability of uniform viscous flow under rollers and spreaders", J. Fluid Mech., vol.7, pp.481.

Zevallos, G. A., M. Pasquali and M.S. Carvalho, 2004, "Film Splitting Flows of Dilute Polymer Solutions", ISCST Symposium, 2004.

5. Responsibility notice

The author(s) is (are) the only responsible for the printed material included in this paper